Exploring time-extended complexity measures in magnetic systems

Jannes van Poppelen
(Dated: October 31, 2023)

Complexity, a fundamental concept in physics, encompasses phenomena spanning atomic to cosmic scales. The natural emergence of complexity can be explained by self-organized criticality. In this work, two complexity measures in magnetic systems are explored. The multiscale structural complexity (MSC) and spin temperature both capture complexity but are fundamentally different in nature and hence behave differently when subject to various temperature profiles. The MSC is extended to incorporate time correlations and compared to the time-averaged static MSC for examining spin glasses and bcc Fe at different temperatures. The spin glass transition temperature is determined with an accuracy of 1 K using the time-extended MSC, outperforming similar estimates based on the heat capacity in terms of accuracy, computational cost, and efficiency. Future work includes the optimization of coarse-graining scales in spin glasses, the investigation of transient magnetization dynamics, and the influence and loss of information of averaging magnetic unit cells before computing complexities.

I. INTRODUCTION

The concept of complexity is a ubiquitous feature in physics, appearing in a diverse range of phenomena from the smallest atomic scales to the largest structures in the universe [1, 2]. Complexity arises from the interactions between the components of a system, leading to the emergence of novel properties that are not readily apparent from the individual components alone. One insightful way to think about this complexity is through the concept of self-organized criticality (SOC) [3, 4]. SOC refers to a state in which the observed complexity emerges in a robust manner, unaffected by fine-tuned details or wide changes in variable parameters within the system. The term "self-organized criticality" captures the idea that critical behavior emerges naturally without the need for precise adjustments. It offers a framework to comprehend how complex systems autonomously reach a state of balance, exhibiting scale-invariant behavior [5]. By encompassing the dynamics of self-organization and criticality, SOC provides insights into the underlying mechanisms of complexity, revealing the intrinsic interdependencies that shape the behavior of complex systems.

The analysis of the multiscale structural complexity (MSC) is another powerful approach for studying complex systems, as it considers the system at multiple scales of organization to gain a comprehensive understanding of its behaviour. The MSC has been extensively analyzed in the study of complex magnetic systems through spin dynamics [6], offering a promising approach for investigating their rich behaviour. Such complex systems often exhibit phase transitions with unknown order parameters [7], making it challenging to understand the underlying physics, however, examining the MSC of the system can help identify relevant correlation lengths and provide insights into the phase transition dynamics.

In this work, the MSC and spin temperature as measures of complexity in magnetic systems are studied through spin dynamics simulations, focusing on bcc Fe. Furthermore, the MSC is extended to include time correlations by treating time as another dimension for coarse-graining and subsequently included in the overlap when computing the complexity. The extended MSC is then compared to the time-averaged static MSC for both spin glasses and bcc Fe for a large range of temperatures to verify its validity. Lastly, spin glass systems are analyzed to gain a deeper understanding of the underlying dynamics of the system, which exhibits complex and disordered magnetic behaviour. While spin glasses are highly frustrated systems, and appear to be random, locally, there is some long-range order in time. The extended MSC capitalizes on their long-range temporal order, whence spin glass transition temperatures are determined. These temperatures are then compared to estimates originating from the heat capacity.

II. THEORY

Coarse-graining is a widely used approach in physics to simplify complex systems by reducing their degrees of freedom [8]. It involves merging small-scale details into a unified entity, resulting in a model that is more convenient and computationally efficient to handle. Coarse-graining also plays a crucial role in the definition of complexity, as it allows for easier comparison of structures at different scales. Definitions and theory regarding the complexity are based on and inspired by [6].

At a scale k, the smallest entity/pixel that can be resolved is denoted by $\mathbf{s}_{ijl}(k)$, which in terms of atomistic spin dynamics represents the magnetic unit cell. Each index of $\mathbf{s}_{ijl}(k)$ then is one of three spin components. Rescaling a coarse-grained entity admits a straightforward way to compute its overlap with different scales.

To put this into perspective, assume a 2D magnetic system can be stored in a 2D matrix, where for the smallest scale $k = 0$, the entire system is represented without any loss of information. Note that the extension to 3D is trivial. At a different, arbitrary scale k, assume the system is represented by a matrix of size $L_{k,x}$ by $L_{k,y}$, which can be further coarse-grained into a matrix using blocks of size Λ_x by Λ_y. The overlap at consecutive scales

is then given by

$$\begin{aligned}\mathcal{O}_{k,k-1} &= \frac{1}{L_{k-1,x}\,L_{k-1,y}} \sum_{i=1}^{L_{k,x}} \sum_{j=1}^{L_{k,y}} \mathbf{s}_{ij}(k) \cdot \\ &\quad \sum_{m=1}^{\Lambda_x} \sum_{l=1}^{\Lambda_y} \mathbf{s}_{\Lambda_x i+m,\Lambda_y j+l}(k-1) \\ &= \frac{\Lambda_x \Lambda_y}{L_{k-1,x}\,L_{k-1,y}} \sum_{i=1}^{L_{k,x}} \sum_{j=1}^{L_{k,y}} \mathbf{s}_{ij}^2(k) \\ &\overset{*}{=} \frac{\Lambda_x \Lambda_y}{L_{k-1,x}\,L_{k-1,y}} \cdot L_{k,x} L_{k,y} \cdot \mathcal{O}_{k,k} = \mathcal{O}_{k,k}.\end{aligned} \tag{1}$$

Here, the step indicated with $\overset{*}{=}$ only holds when coarse-graining is done by averaging, which to a certain extent represents the "mean-field picture". Other schemes for coarse-graining can be used, such as a Gaussian kernel, however, this loses the simplicity of the overlap between the two objects at consecutive scales. Using the overlap at different scales, the complexity for N renormalization steps, i.e. considering N different scales, can be defined as

$$\begin{aligned}\mathcal{C} &= \sum_{k=0}^{N-1} \mathcal{C}_k = \sum_{k=0}^{N-1} |\mathcal{O}_{k+1,k} - \frac{1}{2}(\mathcal{O}_{k,k} + \mathcal{O}_{k+1,k+1})| \\ &\overset{*}{=} \frac{1}{2} \sum_{k=0}^{N-1} |\mathcal{O}_{k+1;k+1} - \mathcal{O}_{k;k}| \\ &\overset{**}{=} \sum_{k=0}^{N-1} |\mathcal{O}_{k+1;k+1} - \mathcal{O}_{k;k}|\end{aligned} \tag{2}$$

Again, the step indicated with $\overset{*}{=}$ only holds when coarse-graining is done by averaging, and the step indicated with $\overset{**}{=}$ is the normalization step. This significantly simplifies the final expression, as it implies overlaps at different scales will not have to be computed. The complexity in the above expression need not be normalized, which does not pose any problems as relative values provide a lot more information than absolute values. However, the complexity has been normalized to allow for comparison between an extension of the complexity which includes time correlations, later on. As a rule of thumb, a complexity of 1 implies a maximally complex state, whereas a complexity of 0 represents a minimally complex state, where the absolute definition of "complex" is relative, and depends on the system that is being studied.

A. Spin temperature and MSC as measures of complexity

Temperature is a different, well-known measure of complexity that is often linked to entropy. Entropy is a representation of the amount of order present in a system. As the temperature rises, so does the entropy, indicating that systems at high temperatures are characterized by disorder.

While the concept of temperature for moving ensembles of particles is well-known and closely connected to the kinetic energy of the particles, the temperature of a spin ensemble is not as well established. In the field of atomistic spin dynamics, the concept of temperature is specifically captured through the spin temperature, which connects temperature to the magnetic moments, $\mathbf{S}_i$, and effective magnetic fields acting on individual atoms, $\mathbf{H}_i$. The main result of [9] is an expression for the spin temperature, which is presented below

$$\begin{aligned}T &= \frac{\mu_s}{2\gamma_s \hbar k_B} = \frac{\left\langle \sum_i |\mathbf{S}_i \times \mathbf{H}_i|^2 \right\rangle}{2k_B \left\langle \sum_i \mathbf{S}_i \cdot \mathbf{H}_i \right\rangle} \\ &= \frac{\left\langle \sum_i |\mathbf{S}_i(t) \times \mathbf{H}_i(t)|^2 \right\rangle_t}{2k_B \left\langle \sum_i \mathbf{S}_i(t) \cdot \mathbf{H}_i(t) \right\rangle_t}.\end{aligned} \tag{3}$$

Spin temperature and the MSC are both measures of order and complexity in magnetic systems, but each of them captures different elements. Spin temperature is a measure of the effective temperature of the magnetic moments of individual atoms. It relates to the distribution of magnetic moments and the strength of the effective magnetic field that each atom experiences and can impact the behaviour of the system in terms of magnetization and susceptibility. In contrast, the MSC captures the complexity of the magnetic system's structure at various length scales. This includes features such as the presence of domains, domain walls, and other structural features that impact the magnetic properties of the system [10].

It is therefore interesting to consider how the MSC compares to the spin temperature in magnetic systems for different temperature profiles: an adiabatic increase of the temperature, a rapid increase of the temperature, or at constant temperatures. Would both measures exhibit a similar response, or would the fundamental differences between the measures manifest themselves?

B. Extending the complexity with time correlations

Although complexity is typically treated as a static quantity, it is intriguing to explore its dynamic behaviour, particularly in the context of spin dynamics. There are, however, multiple possibilities of how to add time dependence to the complexity. The most straightforward approach is to study its time evolution, which has already been extensively analyzed in [6]. While this approach yields intriguing results for transient magnetic systems, it falls short in capturing the long-time correlation/memory exhibited by glassy and frustrated systems [11–13]. Specifically, in spin glasses, there is a tendency for spins to remain in a similar

configuration over time, which is intimately related to the slow dynamics observed in these systems.

To do this, the static complexity has to be extended to include time correlations. While both these ideas attempt to describe the underlying dynamics, they are fundamentally different and hence one should not be expected to reduce into the other in a certain limit or yield similar results. In more detail, the former computes the complexity of a system at each snapshot in time, while the latter computes the complexity between two different time-averaged systems, thereby preserving its multiscale nature, however, now also in time, instead of just space.

Extending the complexity to include time correlations can be achieved as straightforwardly as treating time as an additional dimension to coarse-grain. By adding an extra time scale κ and additional sizes T_κ and Λ_T used for temporal coarse-graining, the spatial overlap can be extended to a spatiotemporal overlap

$$\begin{aligned}
\mathcal{O}_{(\kappa,k);(\kappa-1,k-1)} &= \frac{1}{T_{\kappa-1}\,L_{k-1,x}L_{k-1,y}} \sum_{t=1}^{T_\kappa}\sum_{i=1}^{L_{k,x}}\sum_{j=1}^{L_{k,y}} \\
&\sum_{n=1}^{\Lambda_T}\sum_{m=1}^{\Lambda_x}\sum_{l=1}^{\Lambda_y} \mathbf{s}_{ij;t}(\kappa;k)\cdot \mathbf{s}_{\Lambda i+m,\Lambda j+l;\Lambda_T t+n}(\kappa-1;k-1) \\
&= \frac{\Lambda_x\Lambda_y\Lambda_T}{T_{\kappa-1}\,L_{k-1,x}L_{k-1,y}} \sum_{t=1}^{T_\kappa}\sum_{i=1}^{L_{k,x}}\sum_{j=1}^{L_{k,y}} \mathbf{s}^2_{ij;t}(\kappa;k) \\
&\overset{*}{=} \frac{\Lambda_x\Lambda_y\Lambda_T}{T_{\kappa-1}\,L_{k-1,x}L_{k-1,y}} \cdot L_{k,x}L_{k,y}\,T_\kappa \cdot \mathcal{O}_{(\kappa,k);(\kappa,k)} \\
&= \mathcal{O}_{(\kappa,k);(\kappa,k)},
\end{aligned} \tag{4}$$

where the inner product is extended canonically to the time dimension. The introduction of κ is not necessary, as the temporal coarse-graining could be done at the same scale as the spatial coarse-graining, which essentially yields a 4D spatial complexity (3D in the case of a 2D system). One could argue that this yields a functionally different form than is shown in equation 4, and though this might be the case, it restricts the flexibility too much. The freedom of being able to coarse-grain at different temporal- and spatial scales also opens up for studying more correlation lengths of systems.

The extension of time correlations to the complexity is a bit more intricate and relies on expanding $\mathcal{C}_k$ in a way that is consistent with going back to the finest scale in time, $\kappa \to 0$. Consistent here implies a functional form that corresponds to equation 2, not that $\mathcal{C}_{\kappa,k} \longrightarrow \mathcal{C}_k$. It is possible to enforce that constraint, however, the resulting complexity will then lose its temporal multiscale nature. As such, the temporal scale is added onto $\mathcal{C}_k$ by expanding each overlap $\mathcal{O}$ in equation 2 in κ in a similar way as it appears there, i.e.

$$\begin{aligned}
\mathcal{C}_k \longrightarrow \mathcal{C}_{\kappa,k} \implies \quad & \mathcal{O}_{k+1,k} \longrightarrow \mathcal{O}_{(\kappa+1,k+1);(\kappa,k)} \\
& - \frac{1}{2}\big(\mathcal{O}_{(\kappa,k+1);(\kappa,k)} + \mathcal{O}_{(\kappa+1,k+1);(\kappa+1,k)}\big),
\end{aligned} \tag{5}$$

and likewise for the remaining overlaps. Simplifying by coarse-graining in the mean-field picture, and normalizing the final expression, yields the spatiotemporal complexity

$$\begin{aligned}
\mathcal{C} &= \sum_{\kappa=0}^{N_T-1}\sum_{k=0}^{N-1} \mathcal{C}_{\kappa,k} \\
&= \sum_{\kappa=0}^{N_T-1}\sum_{k=0}^{N-1} \big|\mathcal{O}_{(\kappa+1,k+1);(\kappa+1,k+1)} - \mathcal{O}_{(\kappa,k+1);(\kappa,k+1)} \\
&\qquad + \mathcal{O}_{(\kappa,k);(\kappa,k)} - \mathcal{O}_{(\kappa+1,k);(\kappa+1,k)}\big|
\end{aligned} \tag{6}$$

where N_T is the number of temporal renormalization steps and does not have to equal N.

$\mathcal{C}_{\kappa,k}$ is studied for $\kappa \to 0$ to check for consistency between both the non-normalized complexities

$$\begin{aligned}
\lim_{\kappa\to 0} \mathcal{C}_{\kappa,k} &\overset{!}{\rightsquigarrow} \mathcal{C}_k \\
&= \frac{1}{4}\big|\big(\mathcal{O}_{(1,k+1);(1,k+1)} - \mathcal{O}_{(0,k+1);(0,k+1)}\big) \\
&\qquad - \big(\mathcal{O}_{(1,k);(1,k)} - \mathcal{O}_{(0,k);(0,k)}\big)\big|.
\end{aligned} \tag{7}$$

With the "identification"

$$\frac{1}{2}\big(\mathcal{O}_{(1,k+1);(1,k+1)} - \mathcal{O}_{(0,k+1);(0,k+1)}\big) \rightsquigarrow \mathcal{O}_{k+1,k+1},$$

equation 7 reduces to the correct form, i.e.

$$\lim_{\kappa\to 0} \mathcal{C}_{\kappa,k} \rightsquigarrow \mathcal{C}_k = \frac{1}{2}\big|\mathcal{O}_{k+1,k+1} - \mathcal{O}_{k,k}\big|. \tag{8}$$

Note that the left-hand side on the identification above follows from $\mathcal{C}_0$ in equation 2, as it is the contribution to the complexity on the smallest scale, $k = 0$.
Equations 4 and 6 make up the main result of this work, and extend the static MSC as proposed in [6].

III. RESULTS

Spin dynamics simulations for bcc Fe and spin glasses have been done using the UppASD software package [14, 15]. The simulation boxes are 32 by 32 by 32 unit cells for every simulation. The bcc Fe simulations all contain 2 atoms per magnetic unit cell, except for the adiabatic pulse, which has one iron atom per magnetic unit cell. Simulation temperatures range from far below the Curie temperature to slightly above the Curie temperature to be able to capture the effect of the ferromagnetic to paramagnetic phase transition.

The spin glass systems studied in this work have been simulated according to the Edwards-Anderson model

[16], for which the magnetic Hamiltonian resembles the nearest-neighbour Ising model

$$H = -\sum_{\langle ij \rangle} J_{ij} S_i S_j. \tag{9}$$

Here, the exchange parameters J_{ij} between lattice sites i and j have been randomly sampled from a Gaussian distribution, with the width determining the amount of frustration in the spin glass. The magnetic unit cell in the simulations contains one atom. Edwards-Anderson theory predicts a phase transition from the spin glass phase to a paramagnetic phase at a critical temperature [17], which depends on the level of frustration of the system and hence on the various J_{ij}. A stronger coupling yields stronger frustration between spins, allowing it to compete longer with thermal fluctuations, and thus increasing the critical temperature.

To map each lattice topology to a square or cubic system, each magnetic unit cell has been averaged. For systems that exhibit a more complicated ordering vector, a staggered average should be taken. While it can be argued that the individual magnetic moments represent the smallest entity that can be resolved, analyzing and computing the complexity at this level would have made the task significantly more difficult and tedious. Moreover, averaging the magnetic unit cell is in line with coarse-graining being the general theme for the MSC, and is hence justifiable. Still, averaging the magnetic unit cell comes at the cost of losing information, which for the complexity implies that ferromagnetic and antiferromagnetic systems are equally complex, which is not entirely true. Whether information is lost for other magnetic nanostructures, such as skyrmions, depends mostly on the size of the magnetic unit cell. If the magnetic unit cell is significantly larger than the nanostructure, averaging is more inclined to result in a loss of information, while the converse holds for magnetic unit cells smaller than the nanostructure. While the staggered averaging case has been verified for the case of antiferromagnetic NiO, technical issues prevent the results from contributing to this analysis.

A. Spatial complexity for bcc Fe

For bcc Fe, simulations at constant temperatures yield complexities whose functional form are in good agreement with their respective spin temperatures, as seen in Figures 1 and 2, which, moreover, validates the MSC as a measure of complexity. Interestingly, there is a significant difference in the behaviour of the complexities of the adiabatic temperature pulse, indicated by "pulsed" in the graphs below, and the instantaneous shift in simulation temperature, indicated by "shifted" in the graphs. While both complexities are maximal early on, indicating the presence of the paramagnetic phase, the decrease of the complexity happens at vastly different rates for

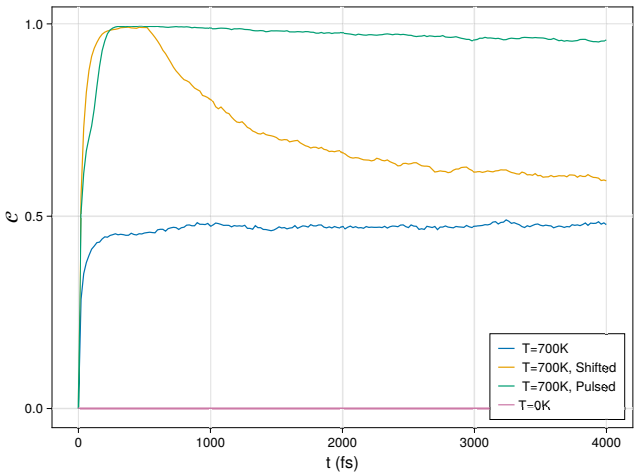

FIG. 1. Complexity for bcc Fe for different temperature profiles. The damping parameter for the simulations is set at 0.3, and spatial complexities are calculated using $\Lambda_x = \Lambda_y = \Lambda_z = 2$, with $N = 3$ renormalization steps.

both processes. For the pulsed temperature profile, the complexity freezes and only slightly decreases for the remainder of the simulation, while the complexity instantly starts to decrease for the shifted temperature profile. It appears as if the complexity thermalizes for adiabatic increases in the temperature.

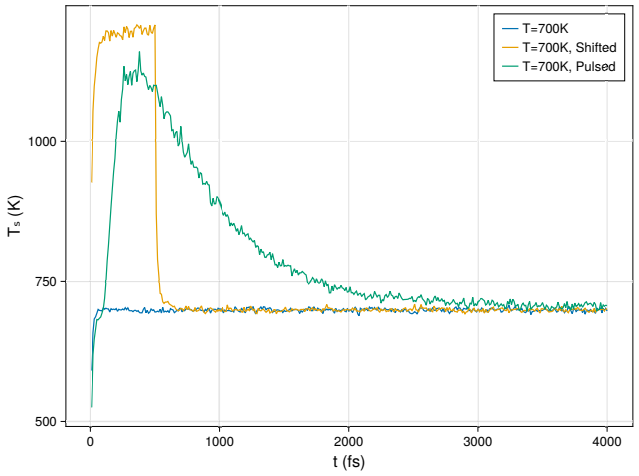

FIG. 2. Spin temperature for bcc Fe for different temperature profiles. The spin temperature for $T = 0$K has been omitted for brevity.

To get a better perspective on what is happening, it is informative to look at the internal energy and the magnetization of both non-constant temperature profiles in Fig 3. The magnetization for both processes vanishes nearly instantly, indicating the arrival of the paramagnetic phase. Upon relaxation of the temperature, the major difference lies in the internal energies, which reveals the formation of local magnetic domains for the shifted

process, but not for the process with adiabatic cooling. This implies that, in a way, the MSC prefers magnetic configurations in which local domains are formed. The fact that the MSC prefers local domains can be well understood from its multiscale nature, through which areas that do not differ locally do not contribute to the complexity and is hence not that surprising. Still, the complexity seems to descend in a similar way as the internal energy, even for the adiabatic process, which captures the fundamental difference between the MSC and the spin temperature as measures of complexity. As such, the MSC can also be used as an abstract measure of relative energy between arbitrary objects, such as images. More practically, the MSC can, for instance, be used to crudely estimate relative internal energies between various materials, at a relatively lower computational cost.

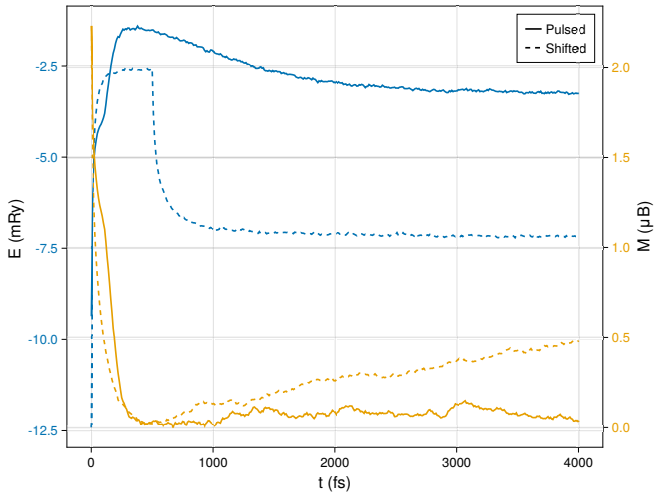

FIG. 3. Internal energy and magnetization for bcc Fe for pulsed (solid) and shifted (dashed) temperature profiles.

The correspondence between MSC and spin temperature can most likely further be improved by relating the spin temperature to the entropy through the heat capacity. Then, with entropy being more intimately related to complexity than spin temperature, the disagreements between MSC and spin temperature should be reduced. Similar investigations have also been done for strongly and weakly damped cases, yielding identical results.

B. Time-extended complexities

The main idea of extending the complexity with time correlations is to be able to check for order there where this is not possible by visual inspection, such as is the case for spin glasses. While they look visibly uncorrelated by eye, there still seem to be, at least locally, correlations in time. Aside from spin glasses, bcc Fe has been simulated at similar temperatures to benchmark the time-extended complexity, as proposed in equation 6. A collection of time-extended and time-averaged complexities for both systems is presented in Fig 4. The same plot with a focus on the low temperatures is presented in Fig 5.

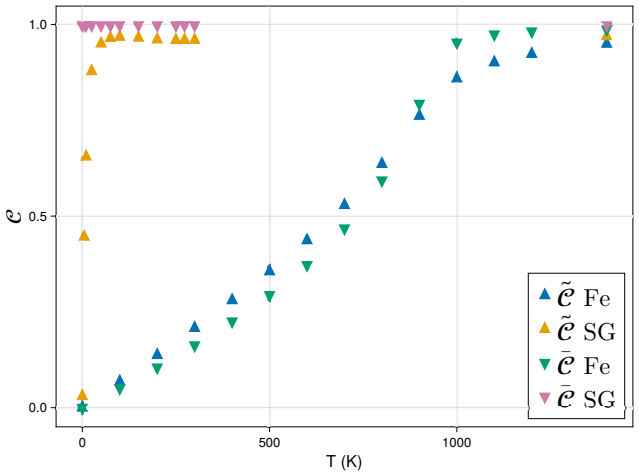

FIG. 4. Temporal complexities for bcc Fe (indicated by Fe) and spin glasses (indicated by SG). Time-extended complexities are given by the inverted triangles, whereas time-averaged spatial complexities are given by regular triangles. Time-extended complexities are calculated using $\Lambda_x = \Lambda_y = \Lambda_z = \Lambda_T = 2$, with $N = 3$ and $N_T = 6$ spatial and temporal renormalization steps, respectively, and time-averaged spatial complexities are calculated using $\Lambda_x = \Lambda_y = \Lambda_z = 2$, with $N = 3$ spatial renormalization steps. Simulations are done with a damping coefficient of 0.3, and the J_{ij} for the spin glass are sampled from a Gaussian with a spread of 0.05.

For the benchmarked case of bcc Fe, it is immediately evident that both the time-extended and time-averaged complexities yield similar results. After all, this system is highly correlated in space. The inclusion of time correlation to the complexity should only slightly increase it, as is the case for the lower temperatures. For temperatures higher than the Curie temperature, this is no longer to be expected, as is observed.

The inclusion of time correlations plays a far larger part in the spin glass system. Here, the time-averaged complexity is maximal for all temperatures, indicating no existence of spatial correlations for spin glasses, i.e., they appear to be completely random at all times, even at 0 K. When time correlations are included, however, the complexity exhibits far more structure, being minimally complex at 0 K, while gradually increasing when the temperature increases. In turn, this implies that, at least locally, spin glasses have a preferred configuration that they do not want to deviate too far from.

The low and high-temperature limits of the time-extended complexities for both systems agree with the physical intuition that at low temperatures there could be some kind of order and that at very high temperatures nothing can exhibit order. The notion that the time-extended complexity is biased for low temperatures, as the dynamics are so slow, is readily nullified, as the frustration in spin glasses yields complex dynamics, which is

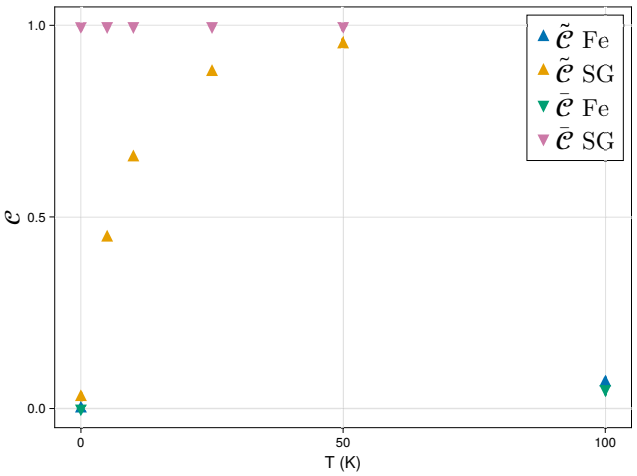

FIG. 5. Closer inspection of the temporal complexities for low temperatures.

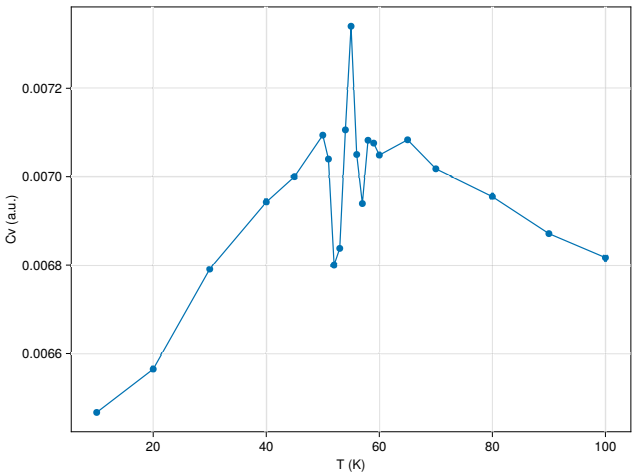

FIG. 6. Heat capacity capturing the spin glass to paramagnetic phase transition. A damping coefficient of 1 has been used to stimulate faster dynamics, and the J_{ij} for the spin glass are sampled from a Gaussian with a spread of 1 to ensure more frustration within the system.

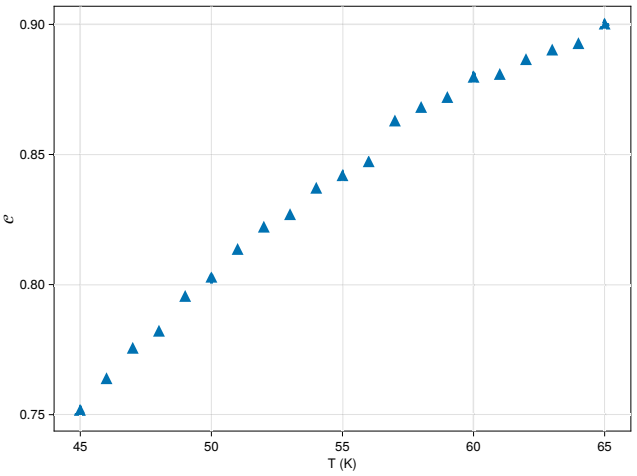

FIG. 7. Time-extended complexity capturing the spin glass to paramagnetic phase transition. Time-extended complexities are calculated using $\Lambda_x = \Lambda_y = \Lambda_z = \Lambda_T = 2$, with $N = 3$ and $N_T = 6$ spatial and temporal renormalization steps, respectively.

still captured.

Having verified the existence of temporal order in the visibly most unordered objects, the next logical step is to exploit the time-extended complexity to investigate whether it is capable of capturing phase transitions that, too, are hard to capture by visual inspection. The most notable example is that of the spin glass to paramagnetic phase transition of the Edwards-Anderson model.

In Fig 6, the heat capacity reveals anomalous behaviour in the 50-65 K range, indicating the spin glass to paramagnetic phase transition. While a cusp in the heat capacity, and likewise, the susceptibility, is a good indicator of the transition temperature, getting a good enough resolution for these is often computationally expensive and hence not that desirable [18].

Instead, by computing the time-extended complexity over a similar range of temperatures, a computationally cheaper, faster, and higher resolution estimate of the transition temperature can be obtained, as seen in Fig 7. The complexity increases at a similar rate until there is a marginal jump between 56 and 57 K. From this temperature on, the nature of the system is completely different. One could argue that the stochastic nature of the spin glass introduces some randomness in the complexity as well. While this is not entirely untrue, the presence of the phase transition around 56 K can be justified by taking a closer look at the relative difference, and hence the derivative, of the complexity.

The derivative of the complexity seems to have a downward trend up to 55 K, after which there is a surge until 57 K, indicating the sudden relative difference in complexities as a result of the phase transition. After 57 K the downward trend seems to persist, with the decline of the derivative indicating a similar magnetic nature of the system. There were attempts to increase the resolution of the complexity between 56 and 57 K, however, the bistable magnetic nature in that range introduced too much randomness in the complexity for it to yield sensible results.

IV. SUMMARY AND CONCLUSION

The MSC and spin temperature for bcc Fe have been compared as measures of complexity. At constant temperatures, both measures are in good agreement with each other. However, there is a significant difference between both measures as a response to adiabatic and instantaneous changes in temperature. The MSC, with its

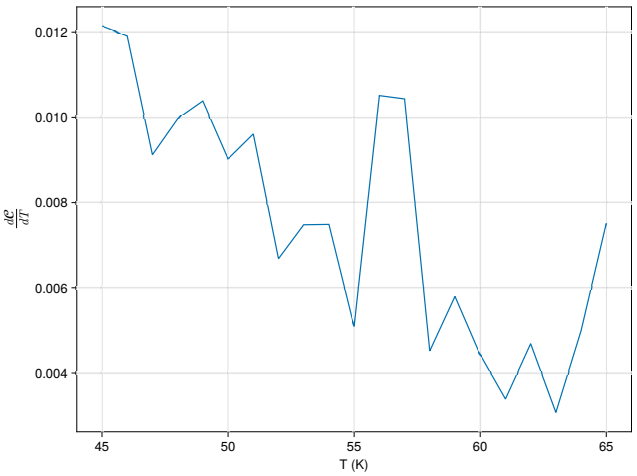

FIG. 8. Derivative of the time-extended complexity.

multiscale nature, prefers configurations that locally look alike, such as the formation of local magnetic domains. It turns out that the MSC can be used to crudely estimate relative energies between various abstract objects of the same kind, which, when investigated further, could prove to be useful when looking for new low-energy materials.

Furthermore, the spatial MSC has been extended to include time correlations to be able to define a complexity for structures that appear random, such as spin glasses. It is shown for bcc Fe that the time-extended complexity behaves in a similar manner as the time-averaged spatial complexity. For spin glasses, time-averaged spatial complexities are maximal for all temperatures, while the time-extended complexity is minimal at 0 K, and increases for increasing temperature, as is physically expected. Using this newly introduced time-extended complexity, the spin glass transition temperature is determined with an accuracy of up to 1 K. Comparing this to estimates using the heat capacity, not only is the complexity analysis far more accurate, but it is also computationally cheaper and faster.

To improve the accuracy of the determination of the spin glass transition temperature, one can experiment with various coarse-graining scales, in both time and space, until satisfactory characteristic lengths are found that lead to improvements. One other possible improvement could be to only consider $\mathcal{C}_{\kappa\geq 0,k>0}$, i.e. omit the contribution from the finest spatial contribution to the complexity, similar to what is done in [6]. It has been attempted in vain, suggesting that significantly larger systems need to be simulated to eliminate the issue of locality. Furthermore, it might be interesting to see how the time-extended complexity responds to transient magnetization dynamics, such as for instance the excitation of magnons. One issue that needs to be further investigated is the influence of averaging magnetic unit cells before computing complexities. Averaging magnetic unit cells leads to the disappearance of exotic nanostructures and consequently the complex physics they entail.

ACKNOWLEDGMENTS

Spin dynamics simulations were enabled by resources provided by the National Academic Infrastructure for Supercomputing in Sweden (NAISS) at NSC partially funded by the Swedish Research Council through grant agreement no. 2022-06725.

[1] A. I. Frenkel, C. W. Hills, and R. G. Nuzzo, The Journal of Physical Chemistry B **105**, 12689 (2001).
[2] A. R. Brown, D. A. Roberts, L. Susskind, B. Swingle, and Y. Zhao, Physical review letters **116**, 191301 (2016).
[3] P. Bak, C. Tang, and K. Wiesenfeld, Physical review A **38**, 364 (1988).
[4] P. Bak, *How nature works: the science of self-organized criticality* (Springer Science & Business Media, 2013).
[5] O. Kinouchi and C. P. Prado, Physical Review E **59**, 4964 (1999).
[6] A. A. Bagrov, I. A. Iakovlev, A. A. Iliasov, M. I. Katsnelson, and V. V. Mazurenko, Proceedings of the National Academy of Sciences **117**, 30241 (2020).
[7] S. Martiniani, P. M. Chaikin, and D. Levine, Phys. Rev. X **9**, 011031 (2019).
[8] E. S. Napolitano, A. Di Renzo, and F. P. Di Maio, Separation and Purification Technology **287**, 120591 (2022).
[9] P.-W. Ma, S. Dudarev, A. Semenov, and C. Woo, Physical Review E **82**, 031111 (2010).
[10] D. Kumar, T. Jin, R. Sbiaa, M. Kläui, S. Bedanta, S. Fukami, D. Ravelosona, S.-H. Yang, X. Liu, and S. Piramanayagam, Physics Reports **958**, 1 (2022).
[11] K. Jonason, E. Vincent, J. Hammann, J. Bouchaud, and P. Nordblad, Physical Review Letters **81**, 3243 (1998).
[12] Y. Joh, R. Orbach, G. Wood, J. Hammann, and E. Vincent, Physical review letters **82**, 438 (1999).
[13] R. Mathieu, P. Jönsson, D. Nam, and P. Nordblad, Physical Review B **63**, 092401 (2001).
[14] J. Hellsvik, L. Bergqvist, A. Bergman, and J. Chico et al, *UppASD*, Uppsala, Sweden (2023).
[15] O. Eriksson, A. Bergman, L. Bergqvist, and J. Hellsvik, *Atomistic spin dynamics: foundations and applications* (Oxford university press, 2017).
[16] S. F. Edwards and P. W. Anderson, Journal of Physics F: Metal Physics **5**, 965 (1975).
[17] J. Chalupa, Solid State Communications **24**, 429 (1977).
[18] C. Mulder, A. Van Duyneveldt, and J. Mydosh, Physical Review B **23**, 1384 (1981).
[19] Y. I. Wolf, M. I. Katsnelson, and E. V. Koonin, Proceedings of the National Academy of Sciences **115**, E8678 (2018).
[20] M. A. Valdez, D. Jaschke, D. L. Vargas, and L. D. Carr, Physical review letters **119**, 225301 (2017).
[21] S. Lloyd, IEEE Control Systems Magazine **21**, 7 (2001).

[22] A. Cole, G. J. Loges, and G. Shiu, Physical Review B **104**, 104426 (2021).
[23] G. M. Whitesides and R. F. Ismagilov, science **284**, 89 (1999).
[24] J. C. Flack and D. C. Krakauer, Chaos: An Interdisciplinary Journal of Nonlinear Science **21**, 037108 (2011).
[25] B. Verlhac, L. Niggli, A. Bergman, U. Kamber, A. Bagrov, D. Iuşan, L. Nordström, M. I. Katsnelson, D. Wegner, O. Eriksson, *et al.*, Nature Physics **18**, 905 (2022).
[26] E. Maletskii, I. Iakovlev, and V. Mazurenko, arXiv preprint arXiv:2302.14558 (2023).